Available online at www.sciencedirect.com
ScienceDirect
Journal of Non-Crystalline Solids 353 (2007) 4344–4352
JOURNAL OF NON-CRYSTALLINE SOLIDS
www.elsevier.com/locate/jnoncrysol

Glass transition and segmental dynamics in poly(dimethylsiloxane)/silica nanocomposites studied by various techniques

Daniel Fragiadakis, Polycarpos Pissis *

Department of Physics, National Technical University of Athens, Zografou Campus, 15780 Athens, Greece

Available online 25 September 2007

Abstract

We report new results on segmental dynamics and glass transition in a series of poly(dimethylsiloxane) networks filled with silica nanoparticles prepared by sol-gel techniques, obtained by differential scanning calorimetry (DSC), thermally stimulated depolarization currents (TSDC), broadband dielectric relaxation spectroscopy (DRS) and dynamic mechanical analysis (DMA). The nanocomposites are characterized by a fine dispersion of 10 nm silica particles and hydrogen bonding polymer/filler interactions. The first three techniques indicate, in agreement with each other, that a fraction of polymer in an interfacial layer around the silica particles with a thickness of 2–3 nm shows modified dynamics. The DSC data, in particular measurements of heat capacity jump at T_g, are analyzed in terms of immobilized polymer in the interfacial layer. The dielectric TSDC and DRS data are analyzed in terms of slower dynamics in the interfacial layer as compared to bulk dynamics. We employ a special version of TSDC, the so-called thermal sampling (TS) technique, and provide experimental evidence for a continuous distribution of glass transition temperatures (T_g) and molecular mobility of the polymer in the interfacial layer, which is consistent with the DRS data. Finally, DMA results show a moderate slowing down of segmental dynamics of the whole polymer matrix (increase of glass transition temperature by about 10 K as compared to the pure matrix).

PACS: 82.35.Np; 64.70.Pf; 77.22.Gm

Keywords: Dielectric properties, relaxation, electric modulus; Glass transition; Nanocomposites; Silica; Polymers and organics; Calorimetry

1. Introduction

Polymer nanocomposites have attracted much interest in recent years for various technological applications, as well as for fundamental research. That is because several properties of the polymer matrix (such as mechanical, thermal and barrier properties) are significantly improved at much lower filler factors, as compared to macro- or micro-scale (conventional) composites [1,2]. Despite many efforts [3,4], there is yet no complete theoretical explanation for this behavior. It is generally accepted, however, that interactions at the polymer–filler interfaces play a significant role. Results obtained by various techniques indicate the presence of an interfacial polymer layer around the filler, with structure/morphology and chain dynamics modified with respect to the bulk polymer matrix [5]. The existence of such an interfacial layer has been postulated for conventional composites long ago and various experiments provided support for that [6]. Questions related to the existence of such an interfacial layer, its thickness and the variation of polymer properties within the layer with respect to bulk properties become crucial for nanocomposites, as the interfacial layer can represent a significant volume fraction of the polymer in nanocomposites. Thus, polymer nanocomposites become interesting also for fundamental studies of interfacial effects. A better understanding of these effects may provide a basis for

* Corresponding author. Tel.: +30 210 7722986; fax: +30 210 7722932.
E-mail address: ppissis@central.ntua.gr (P. Pissis).

0022-3093/$ - see front matter © 2007 Elsevier B.V. All rights reserved.
doi:10.1016/j.jnoncrysol.2007.05.183

understanding (and, thus, tailoring) the improvement of properties at the molecular level.

We may expect that polymeric chains in the vicinity of a solid surface, within a distance of a few nm, exhibit different organization (density, chain conformation) and properties (thermal transitions, molecular mobility), as compared to chains in the bulk [7]. Computer simulations and experiments with model systems provide support for that. Molecular dynamics simulations show that relaxation times may increase or decrease, as compared to the bulk material, depending on the type and strength of interaction and the roughness of the surface. A general result, obtained for a variety of materials and geometries, is that dynamics is similar to that of the bulk material far from the surface (distances larger than a few nm) and changes gradually and significantly (changes of a few orders of magnitude in relaxation times) by approaching the surface [8]. Scheidler et al. [9] proposed an empirical relation for the dependence of relaxation time on the distance from the surface. On the other hand, experiments with model systems, in particular glass forming liquids and polymers confined in porous glasses and thin polymer films, show the presence of additional relaxation processes, a few orders of magnitude slower than the bulk, which are usually discussed in terms of a layer of molecules with reduced mobility at the interface with the solid surface [10].

Results on chain dynamics in polymer nanocomposites, in particular segmental dynamics associated with the glass transition, reported in the literature often appear controversial and confusing [11]: dynamics (often quantified in terms of glass transition temperature) may become faster or slower or show no change, it may be homogeneous or heterogeneous etc. Obviously, several factors, such as polymer–filler interactions, filler size and morphology (degree of dispersion), may affect polymer dynamics in a nanocomposite [12] and should be critically considered. Also, several experimental techniques, including mainly differential scanning calorimetry (DSC) to follow the glass transition, dynamic mechanical analysis (DMA), nuclear magnetic resonance (NMR) and dielectric relaxation spectroscopy (DRS), are typically employed in molecular dynamics studies in polymer nanocomposites. Each of these techniques is characterized by special features, which render it attractive for specific applications, and probes molecular mobility in a different way. This point calls for attention when discussing results obtained by various techniques in terms of chain dynamics.

In the following we focus on polymer/silica, in particular rubber/silica nanocomposites. Experimental results in the literature have often been explained in terms of a three-layer model, originally proposed by Tsagaropoulos and Eisenberg [13] on the basis of DMA results using a variety of matrices, including poly(dimethylsiloxane) (PDMS): a strongly bound, immobile layer immediately surrounding each particle, which does not participate in the glass transition; a second, loosely bound interfacial layer, which is responsible for a second glass transition, 50–100 °C above the bulk glass transition; and the quasi-bulk polymer unaffected by the particles. Results by Kremer and co-workers [14] using DRS and by Litvinov and Spiess [15] using NMR on mixtures of PDMS and aerosils were also interpreted in terms of a three-layer model (strongly bound, loosely bound and quasi-bulk). On the other hand, DMA [16,17] and neutron scattering [18] results obtained with various rubber/silica nanocomposites were explained in terms of a simpler two-layer model: a single interfacial layer with reduced dynamics and quasi-bulk polymer. Finally, DMA results obtained by Long and co-workers [19] on poly(ethyl acrylate)/silica nanocomposites were discussed in terms of a continuous distribution of glass transition temperatures as a function of the distance from the particle surface.

In the framework of a continuing study of PDMS/silica nanocomposites we have already reported on results obtained by broadband dielectric relaxation spectroscopy (DRS) [20,21]. Silica particles had been generated by sol–gel techniques in the presence of cross-linked PDMS and transmission electron microscopy (TEM) images showed an excellent distribution of silica particles in the matrix with a diameter of about 10 nm [22]. In addition to morphology, polymer–filler interactions are also well characterized, as the particles interact with the matrix via hydrogen bonds between the oxygens on the PDMS backbone and the hydroxyls on the silica surface. Thus, we are dealing with a system particularly suited to fundamental studies on interfacial effects on polymer dynamics. In addition to the α relaxation associated with the glass transition (dynamic glass transition) of the polymer matrix, a second slower α relaxation was observed and assigned to polymer chains with restricted dynamics close to the polymer/filler interface. This behavior was discussed in terms of a gradual increase of relaxation times close to the surface of the nanoparticles [21]. Preliminary measurements by DSC and by a second dielectric technique, thermally stimulated depolarization currents (TSDC) were also reported [20]. In this paper we report new results of our investigation. We employ TSDC and a special version of TSDC, the so-called thermal sampling (TS) technique, and provide experimental evidence for a continuous distribution of glass transition temperatures (T_g) and molecular mobility of the polymer in the interfacial layer. Furthermore, we analyze DSC data, in particular measurements of the heat capacity jump at T_g, in terms of immobilized polymer, which does not participate in the glass transition. Finally, we extend our techniques to include DMA, a technique which has been widely used to study rubber/silica nanocomposites [13,16,17], and compare the DMA results with those obtained on the same samples by the thermal and dielectric techniques.

2. Experimental

2.1. Sample preparation

The PDMS/silica nanocomposites were prepared by sol–gel techniques in the presence of cross-linked PDMS using

hydride-terminated precursor chains (covalent bonds between H and Si) and dibutyltin diacetate as a catalyst. Details of the preparation and the results of characterization by SAXS, SANS and TEM have been reported elsewhere [22].

Unfilled PDMS was synthesized from hydrid–terminated PDMS precursor ($M_w = 17{,}200$) with 1,3,5,7-tetravinyl-1,3,5,7-tetramethylcyclotetrasiloxane as cross-linking agent and platinum-divinyltetramethylsiloxane as catalyst. In the in situ filling process, the dried PDMS films were allowed to swell in tetraethoxysilane (TEOS) in the presence of of dibutyltin diacetate as catalyst. Both the TEOS-swollen film and a beaker containing water were then placed for 24 h into a desiccator maintained at a constant temperature (303 K) thus exposing the swollen film to saturated water vapor. The hydrolysis and condensation of TEOS produced the silica phase. Finally, the film was vacuum-dried at 353 K for several days to constant weight. The amount of filler incorporated into the network, controlled by the swelling time of the PDMS samples (films of about 1 mm thickness) in the silica precursor and calculated from their weight before and after the generation of the filler, was varied between 0 and 16 vol.%. Transmission electron microscopy (TEM) images showed a very good dispersion of silica particles with a mean diameter of about 10 nm (Fig. 1 in [22]). In the following samples are designated by PDMSX, where X the volume fraction of silica.

2.2. Experimental Techniques

Differential scanning calorimetry (DSC) measurements (Perkin–Elmer DSC-4 calorimeter) in the temperature range from 110 to 300 K were employed to investigate thermal transitions (glass transition, crystallization and melting events).

Thermally stimulated depolarization currents (TSDC) is a dielectric technique in the temperature domain [23]. The sample is inserted between the plates of a capacitor and polarized by the application of an electric field E_p at temperature T_p for time t_p, which is large compared to the relaxation time of the dielectric relaxation under investigation. With the electric field still applied, the sample is cooled to a temperature T_o, which is sufficiently low to prevent depolarization by thermal energy, and then is short-circuited and reheated at a constant rate b. The discharge current generated during heating is measured as a function of temperature with a sensitive electrometer. TSDC corresponds to measuring dielectric loss at a constant low frequency in the range 10^{-4}–10^{-2} Hz (equivalent frequency). It is characterized by high sensitivity and high resolving power [23]. TSDC measurements were carried out using a Keithley 617 electrometer in combination with a Novocontrol sample cell for TSDC measurements. Typical experimental conditions were 290 K for T_p, 2 kV/cm for E_p, 5 min for t_p, 10 K/min for the cooling rate to $T_o = 120$ K, and 3 K/min for the heating rate b.

Thermal sampling (TS) is a special TSDC technique to experimentally analyze a complex relaxation process into approximately single responses [23]. It consists of 'sampling' the relaxation processes within a narrow temperature range by polarizing at a temperature T_p and depolarizing at T_d, a few degrees lower than T_p. The sample is then cooled down and the depolarization current measured during heating as in standard TSDC. In a series of TS measurements the polarization temperature is varied (here in steps of 5 K) to span the whole temperature range of the complex peak.

Dielectric relaxation spectroscopy (DRS) [24] measurements were carried out in the frequency range 10^{-2}–10^{6} Hz and the temperature range from 140 to 310 K by means of a Novocontrol Alpha analyzer. The temperature was controlled to better than 0.1 K with a Novocontrol Quatro system. At higher frequencies, 10^{6}–10^{9} Hz, measurements were carried out using a Hewlett–Packard 4291A impedance analyzer integrated with a Tabai Espec temperature chamber.

Dynamic mechanical analysis (DMA) measurements were carried out using equipment from polymer laboratories (PL-MK II) at a frequency of 1 Hz in the temperature range 110–300 K.

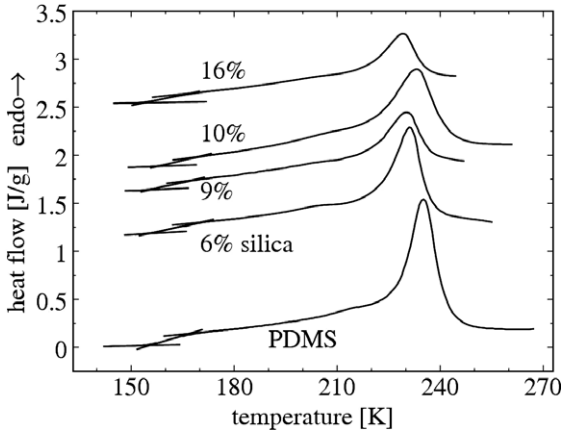

Fig. 1. DSC heating thermograms (second runs, displaced vertically for clarity) obtained with the samples indicated on the plot at a heating rate of 10 K/min after cooling at 10 K/min.

3. Results

Fig. 1 shows DSC heating thermograms of PDMS and four nanocomposites with the filler content (in vol%) indicated on the plot. We observe the glass transition around 160 K and a single endothermic melting peak around 230 K. Here we focus on the glass transition and analyze the corresponding DSC data in terms of glass transition temperature T_g, heat capacity jump ΔC_p at T_g, which is related to the fraction of polymer participating at the glass transition, and the width of transition, related to heterogeneity (Table 1).

T_g shows no significant variation with composition. However, the heat capacity jump at T_g, normalized to the

Table 1
Parameters of the glass transition determined by DSC: Glass transition temperature T_g, onset and end temperatures T_{on} and T_{end}, normalized heat capacity step Δc_p^{norm}, fraction of immobilized polymer χ_{im} and corresponding thickness d_{int} of the immobilized layer

Sample	T_g (K)	T_{on} (K)	T_{end} (K)	Δc_p^{norm} (J/g)	χ_{im}	d_{im} (nm)
PDMS0	160	155	167	0.31	–	–
PDMS6	162	155	170	0.21	0.13	2.3 ± 0.2
PDMS9	162	155	168	0.16	0.20	2.4 ± 0.2
PDMS10	163	155	170	0.17	0.19	2.1 ± 0.2
PDMS16	160	155	167	0.15	0.22	1.6 ± 0.3

fraction of amorphous polymer, Δc_p^{norm}, systematically decreases with increasing filler content (Table 1). Similar results have been obtained also with other polymer nanocomposites and interpreted in terms of a fraction of polymer being immobilized on the surface of the silica particles [25]. This fraction increases with increasing silica content (Table 1). Assuming that the silica nanoparticles are spherical, have a diameter of 10 nm and are statistically distributed in the polymer matrix, the thickness of the immobilized layer is calculated to about 2 nm (Table 1).

Fig. 2 shows TSDC thermograms recorded with pure PDMS and four nanocomposites. The thermogram in pure PDMS shows a single peak at about 150 K, which corresponds to the segmental α relaxation associated with the glass transition of the amorphous phase of PDMS. The temperature T_α of the peak maximum, which is in general a good measure of T_g, is in good agreement with the DSC data. For the nanocomposites the α relaxation is observed at approximately the same temperature, but with a higher intensity due to the decrease in crystallinity. In addition, a shoulder is observed on the high-temperature side of the main peak extending up to approximately 30 K higher. The temperature position of the shoulder is independent of composition, whereas its intensity increases systematically with silica content. The shoulder is assigned to the α relaxation of PDMS chains in an interfacial layer close to the silica particles, where chain mobility is constrained due to interaction with the surface of the particles (hydrogen bonding). This relaxation is referred to in the following as the α′ relaxation. The area of a TSDC peak is proportional to the dielectric strength Δε of the corresponding relaxation [23]

$$\Delta\varepsilon = \frac{Q}{A \cdot \varepsilon_0 \cdot E_P}, \tag{1}$$

where Q is the depolarization charge, determined from the area under the peak, A the surface area of the sample, E_p the polarizing field and ε_0 the vacuum permittivity. The relative areas of the main relaxation and the shoulder give directly the relative volume of the interfacial and bulk phases. For direct comparison the thermograms in the region of the glass transition have been normalized to the same height of the main peak (Fig. 3). The contribution of the shoulder (α′ relaxation, dotted line) is then obtained by subtracting the pure PDMS signal from the normalized nanocomposites signal. The dielectric strength Δε of the α relaxation and of the α′ relaxation is then calculated. The results, listed in Table 2, show that, with increasing silica content, the dielectric strength of the α relaxation decreases in general, whereas that of the α′ relaxation increases approximately linearly. Using the model of interfacial layer, as in the case of DSC data analysis, the fraction of polymer with reduced mobility and the thickness of the interfacial layer are calculated (Table 2). Interestingly, values similar to those calculated from the DSC data are obtained.

At temperatures higher than those of the α and the α′ TSDC peaks a sharp peak is observed in the thermograms of Fig. 2 for all the samples at about 225 K and a broad peak at 250–290 K. The sharp peak is located in the temperature region of the melting (Fig. 1), which in combination with its small width makes it reasonable to associate it

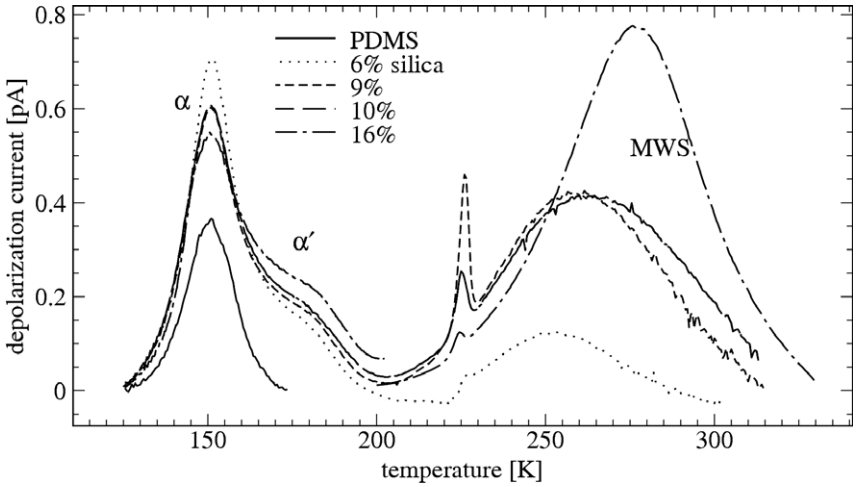

Fig. 2. TSDC themograms for pure PDMS and the four PDMS/silica nanocomposites indicated on the plot.

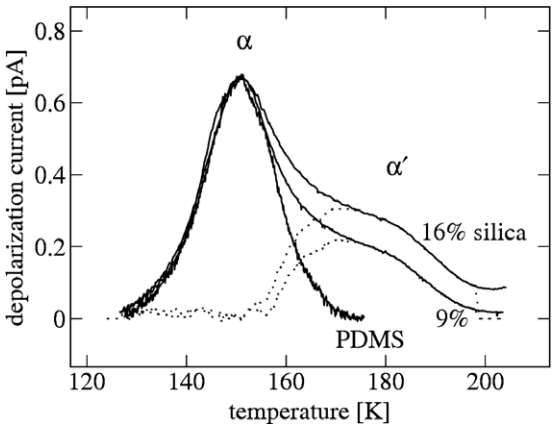

Fig. 3. TSDC thermograms in the region of the glass transition in pure PDMS and two nanocomposites normalized to the temperature and height of the main peak. The dashed line, obtained by subtracting the PDMS thermogram from the nanocomposite thermogram, gives the contribution of the α' relaxation.

Table 2
Normalized dielectric strengths $\Delta\varepsilon_\alpha$ and $\Delta\varepsilon_{\alpha'}$ of the α and α' relaxations, respectively, fraction χ_{int} of interfacial polymer obtained from these and corresponding thickness d_{int} of the interfacial layer

Sample	$\Delta\varepsilon_\alpha$	$\Delta\varepsilon_{\alpha'}$	χ_{int}	d_{int} (nm)
PDMS0	1.12	–	–	–
PDMS6	1.13	0.36	0.13	2.3 ± 0.2
PDMS9	0.88	0.46	0.21	2.5 ± 0.2
PDMS10	0.96	0.55	0.22	2.5 ± 0.2
PDMS16	1.00	0.80	0.29	2.2 ± 0.2

with melting in the crystalline regions of PDMS. The peak originates either from reorientation of dipoles or from release of charges which have been trapped in the interfaces between crystalline and amorphous regions. The broad peak at 250–290 K, which increases in magnitude and shifts to higher temperatures with increasing silica content, is assigned to interfacial Maxwell–Wagner–Sillars (MWS) polarization/relaxation, i.e. to trapping of charge carriers (ions) at interfaces between regions of different conductivity during the polarization step and their release during the depolarization step [23,26].

The TSDC results in Fig. 2 are consistent with both two distinct α and α' relaxations associated with two distinct glass transitions and with a continuous distribution of relaxation times and glass transition temperatures in the interfacial layer. To further follow that question the TS technique [23] was employed. As an example, Fig. 4 shows TS responses (approximately single responses) experimentally isolated in the temperature region of the glass transition in pure PDMS (a) and in the nanocomposites with 10 vol% silica (b). In pure PDMS the TSDC α peak is characterized by a distribution of relaxation times, as commonly found in polymers [27,28]. In the nanocomposites the distribution becomes much broader at higher temperatures (longer relaxation times), corresponding to the region of the shoulder in Fig. 2. Moreover, the magnitude (peak height) of the TS responses decreases continually with increasing polarization temperature and no sign is observed for a second TSDC peak in the temperature region of the shoulder. These results provide strong experimental evidence for a continuous distribution of relaxation times in the glass transition region of the nanocomposites, corresponding to a continuous distribution of T_gs between that of pure PDMS and approximately 190 K. The apparent activation energy E_{act} of the individual TS responses was calculated by the initial rise method [23]

$$\ln J(T) = \text{const} - \frac{E_{act}}{kT}, \tag{2}$$

where J is the depolarization current density, T the temperature and k Boltzmann's constant, and by an approximate expression based on the shape of the peak [29]

$$E_{act} = \frac{T_1 T_m}{7940(T_m - T_1)}, \tag{3}$$

where T_m is the peak temperature, T_1 the temperature on the low-temperature side of the peak at which the current

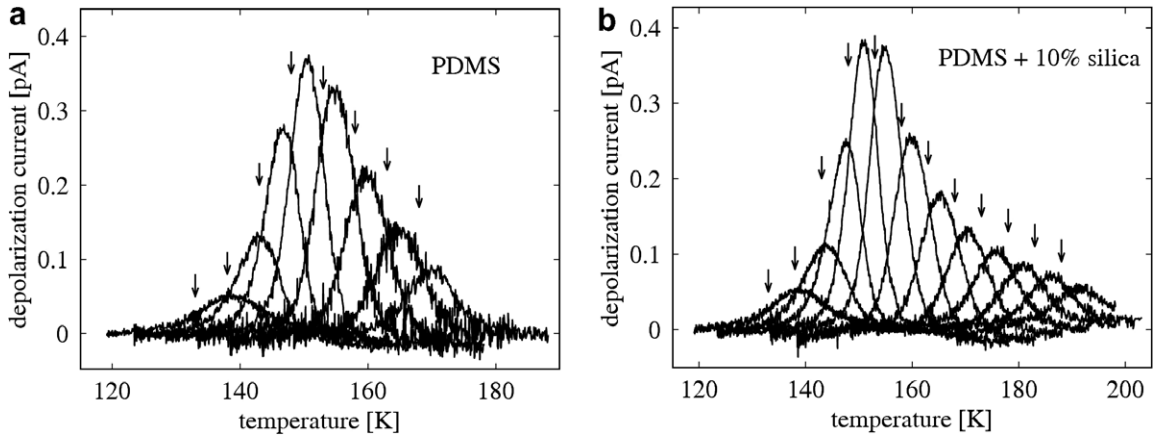

Fig. 4. Thermal sampling responses in the region of the glass transition in pure PDMS and in a nanocomposite. The arrows indicate the polarization temperature for each response.

drops to half its maximum value and E_{act} and T are given in eV and K, respectively. E_{act} is plotted in Fig. 5 as a function of T_p for pure PDMS and one nanocomposite together with the straight line of zero activation entropy corresponding to non-cooperative mechanisms [30]. For pure PDMS the E_{act} values deviate from the straight line for temperatures between $T_g - 15$ and $T_g + 25$ K, indicating the presence of a cooperative relaxation mechanism corresponding to these polarization temperatures. In the nanocomposites the values of E_{act} continue to deviate significantly from the straight line at much higher temperatures (190 K in Fig. 5), indicating the presence of cooperative phenomena in the region of the α' mechanism.

The dynamic glass transition, α and α' relaxations in pure PDMS and the nanocomposites were studied in detail by classical dielectric spectroscopy (DRS) in the frequency domain in [20,21]. To compare with measurements in the temperature domain (DSC, TSDC and later DMA) we show in Fig. 6 DRS results (dielectric loss ε'') measured isothermally in frequency scans and replotted as a function of temperature for pure PDMS and two nanocomposites at three frequencies. A single loss peak is observed in pure PDMS, in agreement with the DRS data in the frequency domain [20,21] shifting to higher temperatures with increasing frequency. In the nanocomposites a double peak is observed, the α loss peak being located at the same temperature as in pure PDMS and the α' loss peak at higher temperatures, becoming more separated and distinguished with increasing frequency.

Dynamic mechanical analysis (DMA) has been widely used to investigate polymer dynamics in rubber/silica nanocomposites [13,16,17]. Fig. 7 shows DMA data obtained with pure PDMS and four nanocomposites: storage modulus E', loss modulus E'' and loss factor $\tan\delta$ ($=E''/E'$) against temperature at a fixed frequency of measurements of 1 Hz. A single peak is observed in E'' and in $\tan\delta$ and a drop in E' in all the samples in the temperature region of the glass transition, the peak in the nanocomposites being shifted by about 10 K to higher temperatures with respect to pure PDMS. At higher temperatures, 180–230 K, E' and E'' decrease gradually, the decrease becoming more pronounced with increasing silica content in the nanocomposites. The steep drop of E' and E'' at 230–240 K is associated with melting in the crystalline regions of PDMS. In the same region a broad peak is observed in $\tan\delta$ which increases in magnitude with increasing silica content. Our interpretation is that this broad peak, not present in $E''(T)$, is related to melting.

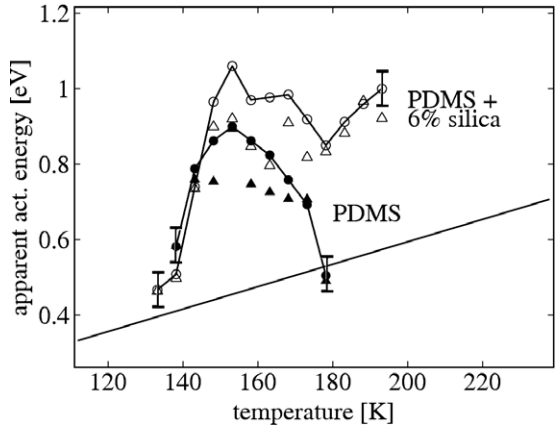

Fig. 5. Apparent activation energy against polarization temperature of the thermal sampling responses of Fig. 4, calculated by Eqs. (2) and (3), circles and triangles, respectively. Full symbols refer to pure PDMS and open symbols to the nanocomposites. The straight line is that of zero activation entropy corresponding to non-cooperative mechanisms [30].

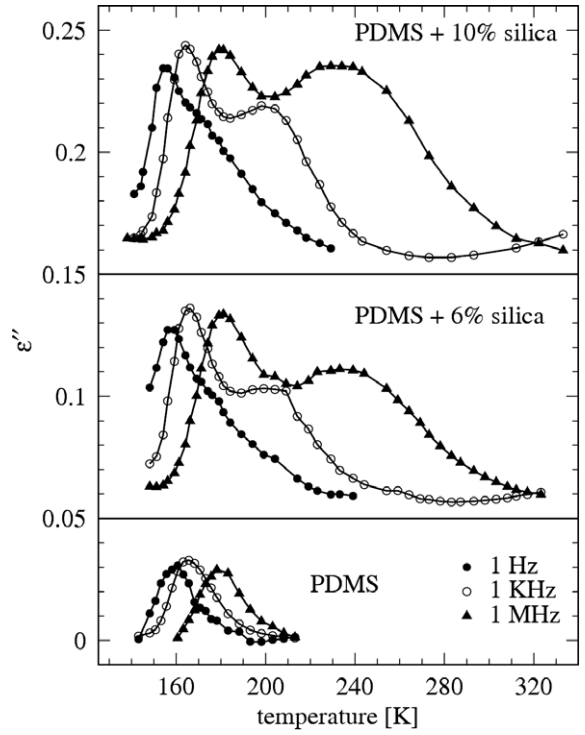

Fig. 6. Dielectric loss ε'' against temperature for pure PDMS and two nanocomposites at three frequencies indicated on the plot.

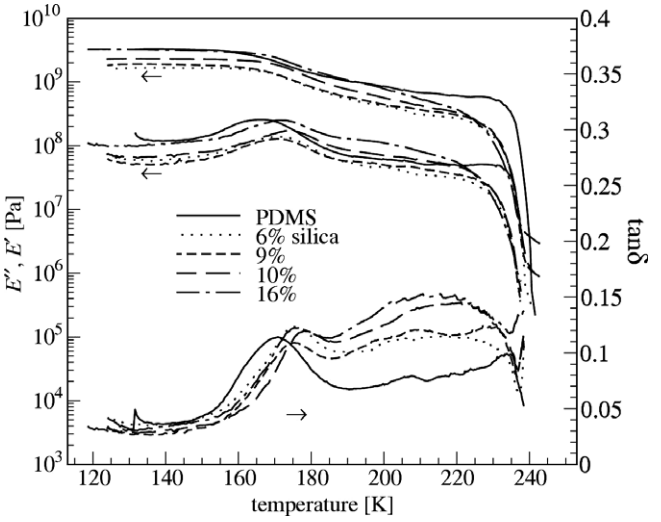

Fig. 7. Mechanical storage modulus E' (upper curves), loss modulus E'' and loss tangent $\tan\delta$ against temperature at 1 Hz of the samples indicated on the plot.

The reduction of chain dynamics in the interfacial layer observed by the other three techniques is here reflected in the shift of the loss peak in the region of the glass transition, i.e. of T_g determined by DMA, to higher temperatures in the nanocomposites as compared to pure PDMS. We will revisit this point in Section 4.

4. Discussion

It is interesting to discuss and compare with each other results for segmental dynamics and glass transition in PDMS and PDMS/silica nanocomposites obtained by the various techniques employed. In agreement with each other the results obtained by all four techniques show clearly that segmental dynamics is reduced in the nanocomposites as compared to pure PDMS within a distance of a few nm from the surface of the nanoparticles. It is essential to note that this clear reduction of mobility is associated with both a fine dispersion of the nanoparticles in the polymer matrix and the existence of hydrogen bonding polymer–filler interactions, as indicated by results obtained with similar series of natural rubber/silica nanocomposites in a related investigation still in progress. The reduced mobility in the nanocomposites is, however, recorded differently by each of the techniques employed.

By DSC a single glass transition is recorded with the same transition temperature T_g for pure PDMS and the nanocomposites. The reduction of molecular mobility in the nanocomposites is reflected in the systematic decrease of the normalized heat capacity jump evaluated in terms of an immobilized interfacial layer with a thickness of about 2 nm (Table 1). The temperature range of the glass transition (T_{end}–T_{on} in Table 1), which is a measure of heterogeneity [25], does not change with composition, providing further evidence that the glass transition recorded by DSC is entirely due to the fraction of unmodified polymer outside the interfacial layer, in agreement with T_g being independent of composition. Results with respect to crystallization and melting were discussed in a previous paper [20], the main conclusion being that the rate of crystallization is reduced in the nanocomposites due to the presence of the silica particles, i.e. slowing down of diffusion dominates over the creation of new crystallization nuclei [1].

The results obtained by TSDC are, in many respects, in agreement with those obtained by DSC, the main difference being that the fraction of polymer recorded as immobilized by DSC gives rise to a slower α' relaxation by TSDC (the shoulder in Fig. 2). At temperatures lower than about 155 K the shape of the α peak is the same in the nanocomposites and in pure PDMS (Fig. 3), providing further support that the dynamics of the chains outside the interfacial layer is not affected by the nanoparticles. Similar values are obtained for the fraction of polymer with reduced dynamics and the corresponding thickness of the interfacial layer by the two techniques. For calculating these values it has been assumed that the interfacial layers of the nanoparticles do not overlap and that the polymer in the interfacial layer does not crystallize (which is reasonable bearing in mind the decrease of crystallinity in the nanocomposites (Fig. 1)). An additional assumption for the TSDC calculations is that the dielectric strength $\Delta\varepsilon$ per unit volume is the same for the α and α' relaxations (Table 2).

The investigation of the interfacial MWS TSDC peak in Fig. 2 may provide, even if indirectly, information on the morphology of the samples. Two kinds of interfaces coexist in the PDMS/silica nanocomposites at low temperatures, those between crystalline and amorphous regions and those between polymer and filler. Since the MWS peak is recorded at temperatures higher than the melting temperature, it must be totally assigned to polymer/filler interfaces. The magnitude of the peak increases significantly for the nanocomposites with the largest (16%) silica content, which might indicate a qualitative change of the morphology for that composition, more likely the existence of polymer regions surrounded by silica nanoparticles resulting in an enhancement of trapping of charge carriers.

The most significant result obtained by TSDC is the experimental evidence for a continuous distribution of glass transition temperatures and of molecular mobility in the nanocomposites provided by the TS technique. It is interesting to note in this connection that attempts to fit the TSDC double peak in the glass transition region (Fig. 2) by a sum of two peaks were not successful [20]. Also, the peak corresponding to the α' mechanism in Fig. 3 does not show the typical shape of a TSDC peak. The values of E_{act} of the TS responses calculated by Eq. (3) are systematically slightly smaller than those calculated by Eq. (2), indicating that the TS responses contain a narrow distribution of activation energies [29]. Also, the values are lower in the region of the shoulder than in the region of the bulk α relaxation, suggesting decreased cooperativity in the region of the shoulder.

The results obtained by DRS provide further support for the TSDC results, indicating the existence of an additional α' relaxation at lower frequencies/higher temperatures than the bulk α relaxation. The α' mechanism corresponds to an interfacial layer with a thickness determined in [21] to be 2–3 nm, decreasing with increasing temperature. The α' loss peak in Fig. 6 becomes more clear and its temperature distance from the α peak increases with increasing frequency. It is interesting to note in this connection the low frequency of DMA measurements (1 Hz) and the even lower equivalent frequency of TSDC and DSC measurements of 10^{-2}–10^{-4} Hz [23,25].

At first glance, there is an apparent inconsistency between the TSDC results, where there is no well-defined second T_g but a continuous distribution, and the DRS results where a distinct second α relaxation (the α' relaxation) is observed at higher temperatures. However, it has been recently demonstrated using computer simulations that a continuous distribution of relaxations times as we approach a solid interface can lead to a double loss peak in the susceptibility, and this has been proposed as an alternative interpretation for this kind of response [9,21].

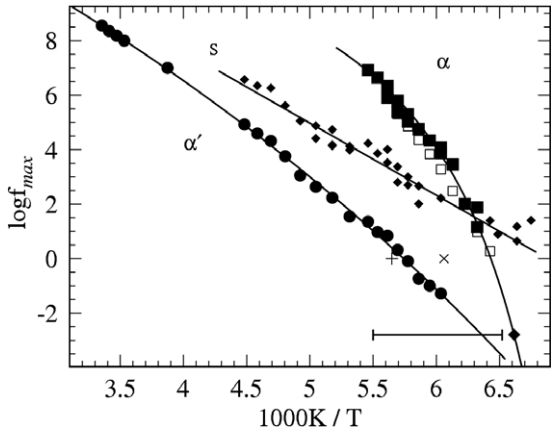

Fig. 8. Arrhenius plot of pure PDMS (open symbols) and the nanocomposite with 9.9 vol.% silica (filled symbols). Included are also TSDC data as a point for α (main peak) and as a horizontal bar for α′ (the shoulder) at the equivalent frequency of 1.6 mHz, and DMA E'' data for pure PDMS (x) and the nanocomposite (+) at 1 Hz. The lines are fits to the DRS data of the Arrhenius equation for the intermediate relaxation and of the Vogel–Tammann–Fulcher equation [21] to the two α relaxations.

DMA data show a different behavior with respect to both DSC and the two dielectric techniques, as only a single peak is observed in the region of the glass transition, both in the loss modulus and in $\tan\delta$, which shifts by about 10 K towards higher temperatures in the nanocomposites (Fig. 7). These results can be understood in terms of a lower spatial resolving power of DMA, at least in the case of our measurements. For comparison, Fig. 8 shows the Arrhenius plot for pure PDMS and a nanocomposite, which was presented and discussed in [21] and has now been enriched with the pure PDMS and the DMA data. The third relaxation s in this plot originates from surface conductivity of silica [14,21]. Please note that for pure PDMS the DMA point is shifted by about 10 K to higher temperatures as compared to the dielectric data, which can be discussed in terms of a different spatial scale of dielectric and mechanical techniques [31]. In a previous work on PDMS/silica nanocomposites using a modified PDMS to prevent crystallization a broad peak in $\tan\delta$ at about 220 K has been interpreted in terms of glass transition of loosely bound polymer [13]. A broad $\tan\delta$ peak recorded with our samples at 210–220 K (Fig. 7) must be associated with melting rather than with a second glass transition, as in that temperature region, the glass transition has been fully completed according to our dielectric data.

5. Conclusions

The main results obtained for polymer dynamics in the PDMS/silica nanocomposites studied and the conclusions can be summarized as follows.

A fraction of polymer close to the silica particles within a distance of a few nm shows modified (slower) dynamics. Different techniques record this modification in different ways: immobilization of polymer in an interfacial layer in DSC (no contribution to heat capacity jump at glass transition), reduced mobility in the interfacial layer in dielectric techniques (a shoulder in TSDC, a second loss peak in DRS), overall reduction of molecular mobility in DMA (a single loss peak shifting, by about 10 K, to higher temperatures in the nanocomposites). In agreement with each other, the thickness of the interfacial layer with modified polymer dynamics is determined by DSC, DRS and TSDC to 2–3 nm at T_g. Preliminary results obtained with other series of rubber/silica nanocomposites indicate that both the fine dispersion of the silica nanoparticles and their strong (hydrogen bonding) interaction with the polymer play an important role in the observed reduction of molecular mobility.

Detailed studies by TSDC, in particular by the thermal sampling technique, provide strong experimental evidence for a continuous distribution of glass transition temperatures as a function of the distance from the silica particle surface, from the bulk T_g at distances larger than 2–3 nm to about 30 K higher at the surface. The thickness of the interfacial layer must then be interpreted as a characteristic distance from the particle surface up to which the effect of the interface reaches. As discussed in a previous paper [21], there is no inconsistency between these results and the DRS results showing a distinct second dynamic glass transition at higher temperatures: it was shown in Ref. [9] that a continuous distribution of relaxation times as we approach the particle surface, which is obtained using computer simulations, can lead to a double loss peak in the susceptibility. With these results in mind, in particular the distribution of $T_g s$ over a temperature range more than 30 K, the question may be raised as to whether more accurate DSC measurements than in the present work (e.g. by using annealing procedures [32] or temperature modulated DSC [33]) would reveal a series of glass transitions in the same temperature range.

Acknowledgements

This work was supported by the Program Archimedes (financed 75% by the European Comission and 25% by the Greek State), as well as by the Greek General Secretariat of Research and Technology (ΠΕΝΕΔ 03ΕΔ150) and the European Social Fund.

References

[1] M. Alexandre, P. Dubois, Mater. Sci. Eng. 28 (2000) 1.
[2] C. Sanchez, G. Soler-Illia, F. Ribot, T. Lalot, C.R. Mayer, V. Cabuil, Chem. Mater. 13 (2001) 3061.
[3] A.C. Balazs, Curr. Opin. Solid St. M. 7 (2003) 27.
[4] K.L. Ngai, Eur. Phys. J. E 12 (2003) 291.
[5] V.M. Litvinov, H. Barthel, J. Weis, Macromolecules 35 (2002) 4356.
[6] C.S. Chouchaoui, M.L. Benzeggagh, Compos. Sci. Technol. 57 (1997) 617.
[7] F. He, L. M. Wang, R. Richert, Phys. Rev. B 71 (2005), Art. No. 144205.

[8] F. Starr, T. Schroder, S. Glotzer, Macromolecules 35 (2002) 4481.
[9] P. Scheidler, W. Kob, K. Binder, J. Phys. Chem. B 108 (2004) 6673.
[10] M. Alcoutlabi, G.B. McKenna, J. Phys. Condens. Mat. 17 (2005) R461.
[11] O. Becker, G.P. Simon, Adv. Polym. Sci. 179 (2005) 29.
[12] S. Merabia, P. Sotta, D. Long, Eur. Phys. J. E 15 (2004) 189.
[13] G. Tsagaropoulos, A. Eisenberg, Macromolecules 28 (1995) 6067.
[14] K. Kirst, F. Kremer, V. Litvinov, Macromolecules 26 (1993) 975.
[15] V. Litvinov, H. Spiess, Macromol. Chem. Phys. 192 (1991) 3005.
[16] V. Arrighi, I. McEwen, H. Qian, M. Prieto, Polymer 44 (2003) 6259.
[17] L. Matejka, O. Dukh, J. Kolarik, Polymer 41 (2000) 1449.
[18] V. Arrighi, J. Higgins, A. Burgess, G. Floudas, Polymer 39 (1998) 6369.
[19] J. Berriot, H. Montes, F. Lequeux, D. Long, P. Sotta, Macromolecules 35 (2002) 9756.
[20] D. Fragiadakis, P. Pissis, L. Bokobza, Polymer 46 (2005) 6001.
[21] D. Fragiadakis, P. Pissis, L. Bokobza, J. Non-Cryst. Solids 352 (2006) 4969.
[22] L. Dewimille, B. Bresson, L. Bokobza, Polymer 46 (2005) 4135.
[23] J. van Turnhout, in: G.M. Sessler (Ed.), Electrets, Topics in Applied Physics, vol. 33, Springer, Berlin, 1980, p. 81.
[24] F. Kremer, A. Schoenhals (Eds.), Broadband Dielectric Spectroscopy, Springer, 2002.
[25] V.A. Bershtein, L.M. Egorova, P.N. Yakushev, P. Pissis, P. Sysel, L. Brozova, J. Polym. Sci. B 40 (2002) 1056.
[26] P. Hedvig, Dielectric Spectroscopy of Polymers, Adam Hilger, Bristol, 1977.
[27] G. Teyssedre, C. Lacabanne, J. Phys. D 28 (1995) 1478.
[28] E. Laredo, A. Bello, M. Grimau, Polym. Bull. 42 (1999) 117.
[29] C. Christodoulides, J. Phys. D 18 (1985) 1501.
[30] H.W. Starkweather, Macromolecules 14 (1981) 1277.
[31] M. Beiner, J. Korus, H. Lockwenz, K. Schroeder, E. Donth, Macromolecules 29 (1996) 5183.
[32] M. Salmeron Sanchez, Y. Touze, A. Saiter, J.M. Saiter, J.L. Gomez Ribelles, Colloid Polym. Sci. 283 (2005) 711.
[33] S. Weyer, H. Huth, C. Schick, Polymer 46 (2005) 12240.